

# Low density ferromagnetism in biased bilayer graphene

Eduardo V. Castro,<sup>1</sup> N. M. R. Peres,<sup>2</sup> T. Stauber,<sup>2,3</sup> and N. A. P. Silva<sup>2</sup>

<sup>1</sup>CFP and Departamento de Física, Faculdade de Ciências Universidade do Porto, P-4169-007 Porto, Portugal

<sup>2</sup>Centro de Física e Departamento de Física, Universidade do Minho, P-4710-057, Braga, Portugal and

<sup>3</sup>Instituto de Ciencia de Materiales de Madrid. CSIC. Cantoblanco. E-28049 Madrid, Spain

(Dated: February 9, 2022)

We compute the phase diagram of a biased graphene bilayer. The existence of a ferromagnetic phase is discussed with respect both to carrier density and temperature. We find that the ferromagnetic transition is first order, lowering the value of  $U$  relatively to the usual Stoner criterion. We show that in the ferromagnetic phase the two planes have unequal magnetization and that the electronic density is hole like in one plane and electron like in the other.

PACS numbers: 73.20.Hb, 81.05.Uw, 73.20.-r, 73.23.-b

*Introduction.*—Graphene, a two-dimensional hexagonal lattice of carbon atoms, has attracted considerable attention due to its unusual electronic properties, characterized by massless Dirac fermions [1, 2]. It was first produced by micromechanical cleavage of graphite and its hallmark is the half integer quantum Hall effect [3].

In addition to graphene, few-layer graphene can also be produced. Of particular interest to us is *bilayer graphene* (BLG), where two carbon planes lay on top of each other according to *AB*-Bernal stacking. In BLG it is possible to have the two planes at different electrostatic potentials. As a consequence, a gap opens at the Dirac point and the low energy band acquires a Mexican hat dispersion [4]. This system is called a biased BLG, and provides the first semiconductor with a gap that can be tuned externally [5, 6, 7]. Due to the Mexican hat dispersion the density of states (DOS) close to the gap diverges as the square root of the energy. The possibility of having an arbitrary large DOS at the Fermi energy poses the question whether this system can be unstable toward a ferromagnetic ground state – a question we want to address in this Letter. From the point of view of the exchange instability, BLG was found to be always unstable toward a ferromagnetic ground state for low enough densities [8, 9].

The question of magnetism in carbon based systems has already a long history. Even before the discovery of graphene, graphite has attracted a broad interest due to the observation of anomalous properties, such as magnetism and insulating behavior in the direction perpendicular to the planes [10, 11, 12, 13, 14]. The research of *s* – *p* based magnetism [15, 16, 17] was especially motivated by the technological use of nanosized particles of graphite, which show interesting features depending on their shape, edges, and applied field of pressure [18]. Microscopic theoretical models of bulk carbon magnetism include nitrogen-carbon compositions where ferromagnetic ordering of spins could exist in  $\pi$  delocalized systems due to a lone electron pair on a trivalent element [19] or intermediate graphite-diamond structures where the alternating  $sp^2$  and  $sp^3$  carbon atoms play the role

of different valence elements [20]. More general models focus on the interplay between disorder and interaction [21, 22]. Further, midgap states due to zigzag edges play a predominant role in the formation of magnetic moments [23, 24] which support flat-band ferromagnetism [25, 26, 27]. Magnetism is also found in fullerene based metal-free systems [28]. For a recent overview on metal-free carbon based magnetism see Ref. [29].

*Model and mean field treatment.*—Due to the electrostatically invoked band-gap, there is a large DOS for low carrier density and thus effective screening of the Coulomb interaction. Coulomb interaction shall thus be treated using a Hubbard on-site interaction.

The Hamiltonian of a biased BLG Hubbard model is the sum of two pieces  $H = H_{TB} + H_U$ , where  $H_{TB}$  is the tight-binding part and  $H_U$  is the Coulomb on-site interaction part. The term  $H_{TB}$  is a sum of four terms: the tight-binding Hamiltonian of each plane, the hopping term between planes, and the applied electrostatic bias. We therefore have  $H_{TB} = \sum_{\ell=1}^2 H_{TB,\ell} + H_{\perp} + H_V$ , with  $H_{TB,\ell} = -t \sum_{\mathbf{r},\sigma} a_{\ell\sigma}^\dagger(\mathbf{r}) [b_{\ell\sigma}(\mathbf{r}) + b_{\ell\sigma}(\mathbf{r} - \mathbf{a}_1) + b_{\ell\sigma}(\mathbf{r} - \mathbf{a}_2)] + h.c.$ ,  $H_{\perp} = -t_{\perp} \sum_{\mathbf{r},\sigma} [a_{1\sigma}^\dagger(\mathbf{r}) b_{2\sigma}(\mathbf{r}) + h.c.]$ , and  $H_V = \frac{V}{2} \sum_{\mathbf{r},x,\sigma} [n_{x1\sigma}(\mathbf{r}) - n_{x2\sigma}(\mathbf{r})]$ . The term  $H_U$  is given by  $H_U = U \sum_{\mathbf{r},x} [n_{x1\uparrow}(\mathbf{r}) n_{x1\downarrow}(\mathbf{r}) + n_{x2\uparrow}(\mathbf{r}) n_{x2\downarrow}(\mathbf{r})]$ . We used  $n_{x\ell\sigma}(\mathbf{r}) = x_{\ell\sigma}^\dagger(\mathbf{r}) x_{\ell\sigma}(\mathbf{r})$ ,  $x = a(b)$ , as the number operator at position  $\mathbf{r}$  and sublattice  $A\ell$  ( $B\ell$ ) of layer  $\ell = 1, 2$ , for spin  $\sigma = \uparrow, \downarrow$ ;  $\mathbf{a}_1 = a(1, 0)$  and  $\mathbf{a}_2 = a(1, -\sqrt{3})/2$  are the basis vectors and  $a \approx 2.46 \text{ \AA}$  the lattice constant. Unless stated otherwise, we use  $t = 2.7 \text{ eV}$ ,  $t_{\perp} = 0.2t$ , and  $V = 0.05 \text{ eV}$  [30].

The problem defined by  $H_{TB} + H_U$  cannot be solved exactly. We adopt a mean field approach, recently applied to describe magnetic properties of graphene nanolands [31]. Since the two planes of the BLG are at different electrostatic potentials, we expect an asymmetry between layers for the charge density  $n$  and the magnetization  $m = n_{\uparrow} - n_{\downarrow}$  (per unit cell). Accordingly, we propose the following broken symmetry ground state, which also defines the mean field parameters:  $\langle n_{x1\sigma}(\mathbf{r}) \rangle = \frac{n+\Delta n}{8} + \sigma \frac{m+\Delta m}{8}$  and  $\langle n_{x2\sigma}(\mathbf{r}) \rangle = \frac{n-\Delta n}{8} + \sigma \frac{m-\Delta m}{8}$ ,

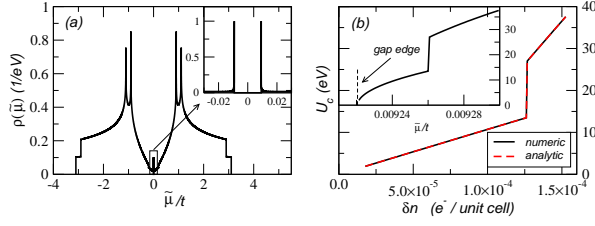


FIG. 1: (Color online) (a) Bilayer graphene DOS for  $U = 0$ . Inset: Zoom near the gap region. (b)  $U_c$  vs  $\delta n$  in the low doping regime. Inset: The same as a function of  $\tilde{\mu}$ .

where  $\Delta n$  and  $\Delta m$  represent the charge density and the spin polarization difference between the two layers, respectively [32]. This leads to an effective bias  $V_\sigma = V + U\Delta n/4 - \sigma U\Delta m/4$ .

If one assumes the ferromagnetic transition to be second order, with  $m = 0$  and  $\Delta m = 0$  at the transition, we are lead to a  $U$ –critical  $U_c$  given by,

$$U_c = 1/\rho_b(\tilde{\mu}, U_c), \quad (1)$$

where  $\rho_b(\tilde{\mu}, U_c)$  is the DOS per spin per lattice point and  $\tilde{\mu} = \mu - nU_c/8$ , with chemical potential  $\mu$ . Although Eq. (1) looks like the usual Stoner criterion, the effective bias  $V_\sigma$  depends on  $U$  due to  $\Delta n$ . This makes Eq. (1) non-linear, and  $U_c$  has to be found numerically in a self-consistent way.

*Simple results.*—We start with the zero temperature ( $T = 0$ ) phase diagram in the plane  $U$  vs  $\delta n$ , where  $\delta n$  is the doping relatively to the half filled case. An approximate analytic treatment is possible in this limit, which is used to check our numerical results.

In Fig. 1 (a) we represent the DOS of a biased BLG with  $U = 0$ . As seen in the inset, the DOS diverges at the edges of the gap. As a consequence, the closer the chemical potential to the gap edges, the lower the critical  $U_c$  value. The low doping  $U_c$  value – given by Eq. (1) in the limit  $U\Delta n \ll V$  – is shown in Fig. 1 (b), both as a function of  $\delta n$  and  $\tilde{\mu}$  (inset). The lowest represented value of  $U_c$  is about  $U_c \simeq 2.7$  eV to which corresponds  $\delta n \simeq 2.5 \times 10^{-5}$  electrons per unit cell. The step like discontinuity shown in panel (b) for  $U_c$  occurs when the Fermi energy equals  $V/2$ , signaling the top of the Mexican hat dispersion relation.

It is clear from Fig. 1 (b) that in the low doping limit  $U_c$  is a linear function of  $\delta n$ . To understand this behavior, first we note that for very low doping the DOS close to the gap edges behaves as  $\rho_b(\tilde{\mu}) \propto (|\tilde{\mu}| - \Delta_g/2)^{-1/2}$ , where  $\Delta_g$  is the size of the gap. Using this approximate expression to compute the doping,  $\delta n \propto \text{sign}(\tilde{\mu}) \times \int_{\Delta_g/2}^{|\tilde{\mu}|} dx \rho_b(x)$ , we immediately get  $\delta n \propto \text{sign}(\tilde{\mu})/\rho_b(\tilde{\mu})$  and thus  $U_c \propto |\delta n|$ . In Fig. 1 (b) both the numerical result of Eq. (1) and the approximated analytical result just derived are shown. The agreement is excellent.

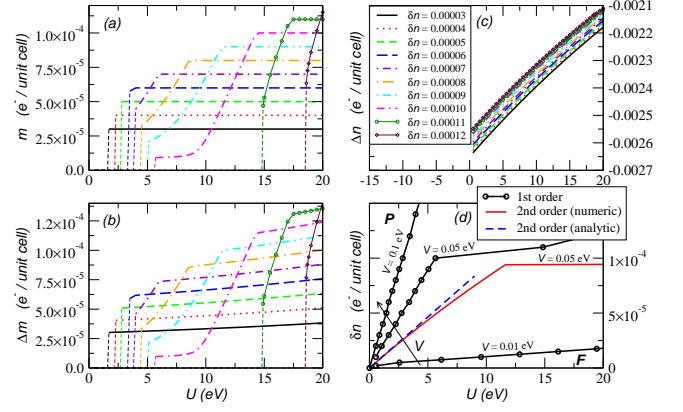


FIG. 2: (Color online) Panels (a), (b), and (c) show the  $T = 0$  solution for  $m$ ,  $\Delta m$ , and  $\Delta n$ , respectively. Panel (d) shows the  $U$  vs  $\delta n$  phase diagram at  $T = 0$ : symbols are inferred from panel (a) and signal a *first-order* transition; lines stand for the *second-order* one given by Eq. (1). Labels:  $P$ -paramagnetic,  $F$ -ferromagnetic.

*Self-consistent solution.*—In order to obtain the  $T = 0$  phase diagram of the biased BLG, we study how  $m$ ,  $\Delta m$ , and  $\Delta n$  depend on the interaction  $U$ , for given values of the electronic doping  $\delta n$ .

In Fig. 2 (a) it is shown how  $m$  depends on  $U$  for different values of  $\delta n$ . The chosen values of  $\delta n$  correspond to the chemical potential being located at the divergence of the low energy DOS, which explains the smaller critical  $U_c$  value for smaller  $\delta n$ . It is interesting to note that the saturation values of the magnetization correspond to full polarization of the doping charge density with  $m = \delta n$ , also found within a one-band model [9]. In Fig. 2 (b) we plot the  $\Delta m$  vs  $U$ . Interestingly, the value of  $\Delta m$  vanishes at the same  $U_c$  as  $m$ . For finite values of  $m$  we have  $\Delta m > m$ , which means that the magnetization of the two layers is opposite and unequal. In Fig. 2 (c) we show  $\Delta n$  vs  $U$ . It is clear that  $|\delta n| < |\Delta n|$ , which implies that the density of charge carriers is above the Dirac point in one plane and below it in the other plane. This means that the charge carriers are electron like in one plane and hole like in the other. As  $U$  is increased  $\Delta n$  is suppressed in order to reduce the system Coulomb energy.

In Fig. 2 (d) we show the  $T = 0$  phase diagram in the  $U$  vs  $\delta n$  plane. Here we concentrate on the  $V = 0.05$  eV case. Symbols are inferred from the magnetization in panel (a). They signal a *first-order* transition when  $m$  increases from zero to a finite value [see panel (a)]. The full (red) line is the numerical self-consistent result of Eq. (1), and the dashed (blue) line is the approximate analytic result described above. The discrepancy between lines and symbols has a clear meaning. In order to obtain Eq. (1) we assumed that a *second-order* transition would take place. This is not the case, and the system under-

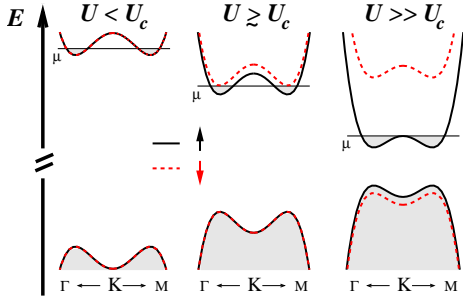


FIG. 3: (Color online) Hartree-Fock bands for  $\uparrow$  (full lines) and  $\downarrow$  (dashed lines) spin polarizations.

goes a first-order transition for smaller  $U$  values. There are clearly two different regimes: one for  $\delta n \lesssim 10^{-4}$ , where the dependence of  $\delta n$  on  $U_c$  is linear, and another for  $\delta n > 10^{-4}$ , where a plateau like behavior develops. This plateau has the same physical origin as the step like discontinuity we have seen in Fig. 1 (b). In the limit  $\delta n \rightarrow 0$  we have not only  $U_c \rightarrow 0$ , but also  $m \rightarrow 0$  and  $\Delta m \rightarrow 0$  [see panels (a) and (b) of Fig. 2], implying a *paramagnetic* ground state for the undoped biased BLG.

Figure 2 (d) shows also the effect of  $V$  on the  $T = 0$  phase diagram (the effect of  $t_\perp$  being similar). Raising either  $V$  or  $t_\perp$  leads to a decrease of the critical- $U$  needed to establish the ferromagnetic phase for a given  $\delta n$ . The order of the transition, however, remains *first-order*. We have observed that decreasing  $t_\perp$  leads to a decrease in  $\Delta m$ , and below some  $t_\perp$  we can have  $\Delta m < m$ . A similar effect has been seen when  $V$  is increased. It should be noted, however, that  $m$  and  $\Delta m$  are  $U$ -dependent, meaning that, depending on  $V$  and  $t_\perp$ , we can go from  $\Delta m < m$  to  $\Delta m > m$  just by increasing  $U$ . Irrespective of  $V$  and  $t_\perp$  we have always observed  $|\delta n| < |\Delta n|$ : electron like carriers in one plane and hole like in the other.

*Understanding the asymmetry between planes.*—The asymmetry between planes regarding both charge and spin polarization densities can be understood based on the Hartree-Fock bands shown in Fig. 3. Additionally, we note that in the biased BLG the weight of the wave functions in each layer for near-gap states is strongly dependent on their valence band or conduction band character [6, 33, 34]. Valence band states near the gap are mostly localized on layer 2, due to the lower electrostatic potential  $-V/2$ . On the other hand, near-gap conduction band states have their highest amplitude on layer 1, due to the higher electrostatic potential  $+V/2$ .

The case  $U < U_c$  shown in Fig. 3 (left) stands for the paramagnetic phase. The values  $m = 0$  and  $\Delta m = 0$  are an immediate consequence of the degeneracy of  $\uparrow$  and  $\downarrow$  spin polarized bands. The presence of a finite gap, however, leads to the abovementioned asymmetry between near-gap valence and conduction states. As a consequence, a half-filled BLG would have  $n_2 = (4 +$

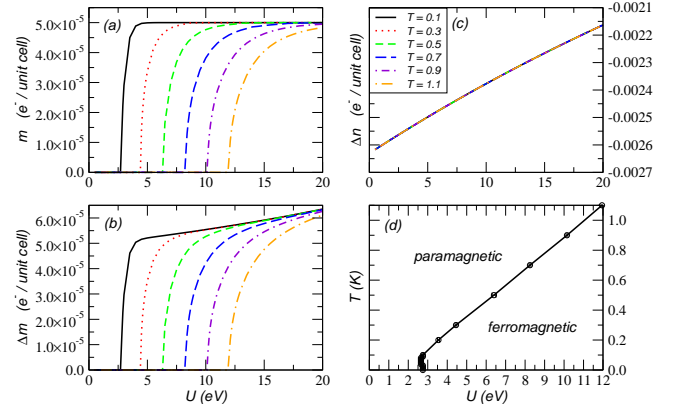


FIG. 4: (Color online) Panels (a), (b), and (c) show the finite  $T$  solution for  $m$ ,  $\Delta m$ , and  $\Delta n$ , respectively, with  $T$  measured in K. Panel (d) shows the  $U$  vs  $T$  phase diagram.

$\Delta n)/2$   $e^-/\text{unit cell}$  on layer 2 (electron like carriers) and  $n_1 = (4 - \Delta n)/2$   $e^-/\text{unit cell}$  on layer 1 (hole like carriers), with  $\Delta n \neq 0$ . Even though the system is not at half-filling, as long as  $|\delta n| < |\Delta n|$  the carriers on layers 1 and 2 will still be hole and electron like, respectively.

Let us now consider the case  $U \gtrsim U_c$  shown in Fig. 3 (center). The degeneracy lifting of spin polarized bands gives rise to a finite magnetization,  $m \neq 0$ . Interestingly enough, the degeneracy lifting is only appreciable for conduction bands, as long as  $U$  is not much higher than  $U_c$ . This explains why we have  $m \approx \Delta m$ , as shown in panels (a) and (b) of Fig. 2 – as only conduction bands are contributing to  $\Delta m$ , the spin polarization density is almost completely localized in layer 1, where  $m_1 = (m + \Delta m)/2 \approx m$ , while the spin polarization in layer 2 is negligible,  $m_2 = (m - \Delta m)/2 \approx 0$ .

It is only when  $U \gg U_c$  that valence bands become non-degenerate, as seen in Fig. 3 (right). This implies that near-gap valence states with  $\uparrow$  and  $\downarrow$  spin polarization have different amplitudes in layer 2. As the valence band for  $\downarrow$  spin polarization has a lower energy the near-gap valence states with spin  $\downarrow$  have higher amplitude in layer 2 than their spin  $\uparrow$  counterparts. Consequently, the magnetization in layer 2 is effectively opposite to that in layer 1, i.e.,  $\Delta m > m$ , as can be observed in panels (a) and (b) of Fig. 2.

We note that the cases  $U \gtrsim U_c$  and  $U \gg U_c$  are parameter dependent. The valence bands can show an appreciable degeneracy lifting already for  $U \gtrsim U_c$ , especially for small values of the  $t_\perp$  parameter. In this case the magnetization of the two layers is no longer opposite, with  $\Delta m < m$ . This can be understood as due to the fact that as  $t_\perp$  is decreased the weight of near-gap wave functions becomes more evenly distributed between layers, leading not only to a decrease in  $\Delta n$  but also in  $\Delta m$ .

*Finite temperature.*—Now we describe the phase diagram of the biased BLG in the  $T$  vs  $U$  plane. This is done in Fig. 4 for  $\delta n = 5 \times 10^{-5}$   $e^-/\text{unit cell}$ . For

$T = 0 - 1.1$  K we studied the dependence of  $m$ ,  $\Delta m$  and  $\Delta n$  on the interaction  $U$ . First we note that the minimum critical- $U$  is not realized at  $T = 0$ . There is a reentrant behavior which is signaled by the smallest  $U_c$  for  $T = 0.06 \pm 0.02$  K. For temperatures above  $T \approx 0.1$  K we have larger  $U_c$  values for the larger temperatures, as can be seen in panel (a). The same is true for  $\Delta m$  in panel (b). As in the case of Fig. 2, the value of  $\Delta m$ , at a given  $T$  and  $U$ , is larger than  $m$ . Also the value of  $\Delta n$ , shown in panel (c), is larger than  $\delta n$ . Therefore we have the two planes presenting opposite magnetization and the charge carriers being hole like in one graphene plane and electron like in the other. In panel (d) of Fig. 4 we present the phase diagram in the  $U$  vs  $T$ . Except at very low temperatures, there is a linear dependence of  $U_c$  on  $T$ . It is clear that at low temperatures,  $T \simeq 0.2$  K, the value of  $U_c$  is smaller than the estimated values of  $U$  for carbon compounds [35, 36].

*Disorder.*—Crucial prerequisite in order to find ferromagnetism is a high DOS at the Fermi energy. The presence of disorder will certainly cause a smoothing of the singularity in the DOS and the band gap renormalization, and can even lead to the closing of the gap. We note, however, that for small values of the disorder strength the DOS still shows an enhanced behavior at the band gap edges [37]. The strong suppression of electrical noise in BLG [38] further suggests that in addition to a high crystal quality – leading to remarkably high mobilities [39] – an effective screening of random potentials is at work. Disorder should thus not be a limiting factor in the predicted low density ferromagnetic state, as long as standard high quality BLG samples are concerned.

Let us also comment on the next-nearest interlayer-coupling  $\gamma_3$ , which in the unbiased case breaks the spectrum into four pockets for low densities [40]. In the biased case,  $\gamma_3$  still breaks the cylindrical symmetry, leading to the trigonal distortion of the bands, but the divergence in the density of states at the edges of the band gap is preserved [37]. Therefore, the addition of  $\gamma_3$  to the model does not qualitatively change our result.

*Conclusion.*—We have found that in the ferromagnetic phase the two layers in general have opposite magnetization and that the electronic density is hole like in one plane and electron like in the other. We have also found that at zero temperature, where the transition can be driven by doping, the phase transition between paramagnetic and ferromagnetic phases is *first-order*.

EVC, NMRP and TS acknowledge the financial support from POCI 2010 via project PTDC/FIS/64404/2006, the ESF Science Program

INSTANS. This work has also been supported by MEC (Spain) through Grant No. FIS2004-06490-C03-00, by the European Union, through contract 12881 (NEST), and the Juan de la Cierva Program (MEC, Spain).

- 
- [1] A. H. Castro Neto *et al.*, arXiv:0709.1163 (to appear in Rev. Mod. Phys.).
  - [2] M. I. Katsnelson, Mater. Today **10**, 20 (2007).
  - [3] A. K. Geim *et al.*, Nat. Mater. **6**, 183 (2007).
  - [4] F. Guinea *et al.*, Phys. Rev. B **73**, 245426 (2006).
  - [5] T. Ohta *et al.*, Science **312**, 951 (2006).
  - [6] E. V. Castro *et al.*, Phys. Rev. Lett. **99**, 216802 (2007).
  - [7] J. B. Oostinga *et al.*, Nature Mater. **7**, 151 (2007).
  - [8] J. Nilsson *et al.*, Phys. Rev. B **73**, 214418 (2006).
  - [9] T. Stauber *et al.*, Phys. Rev. B **75**, 115425 (2007).
  - [10] P. Esquinazi *et al.*, Phys. Rev. B **66**, 024429 (2002).
  - [11] H. Kempa *et al.*, Phys. Rev. B **65**, 241101(R) (2002).
  - [12] H. Kempa *et al.*, Solid State Commun. **125**, 1 (2003).
  - [13] Y. Kopelevich *et al.*, Phys. Rev. Lett. **90**, 156402 (2003).
  - [14] H. Ohldag *et al.*, Phys. Rev. Lett. **98**, 187204 (2007).
  - [15] A. V. Rode *et al.*, Phys. Rev. B **70**, 054407 (2004).
  - [16] P. Turek *et al.*, Chem. Phys. Lett. **180**, 327 (1991).
  - [17] V. I. Srdanov *et al.*, Phys. Rev. Lett. **80**, 2449 (1998).
  - [18] T. Enoki *et al.*, J. Mater. Chem. **15**, 3999 (2005).
  - [19] A. A. Ovchinnikov, Theor. Chem. Acta **47**, 297 (1978).
  - [20] A. A. Ovchinnikov and I. L. Shamovsky, J. Mol. Struct. (Theochem) **251**, 133 (1991).
  - [21] T. Stauber *et al.*, Phys. Rev. B **71**, 041406(R) (2005).
  - [22] M. A. H. Vozmediano *et al.*, Phys. Rev. B **72**, 155121 (2005).
  - [23] M. Fujita *et al.*, J. Phys. Soc. Jpn. **65**, 1920 (1996).
  - [24] L. Pisani *et al.*, Phys. Rev. B **75**, 064418 (2007).
  - [25] A. Mielke, J. Phys. A **24**, L73 (1991).
  - [26] H. Tasaki, Prog. Theor. Phys. **99**, 489 (1998).
  - [27] K. Kusakabe *et al.*, Phys. Rev. B **67**, 092406 (2003).
  - [28] J. A. Chan *et al.*, Phys. Rev. B **70**, 041403(R) (2004).
  - [29] *Carbon Based Magnetism*, edited by T. Makarova and F. Palacio (Elsevier, Amsterdam, 2006).
  - [30] We assume that  $V$  and the charge density are independent and can be externally controlled [7].
  - [31] J. Fernandez-Rossier and J. J. Palacios, Phys. Rev. Lett. **99**, 177204 (2007).
  - [32] Assuming equal spin densities in sublattices  $A$  and  $B$  of the same layer is a reasonable approximation for  $t_{\perp} \ll t$ .
  - [33] E. McCann, Phys. Rev. B **74**, 161403(R) (2006).
  - [34] H. Min *et al.*, Phys. Rev. B **75**, 155115 (2007).
  - [35] R. G. Parr *et al.*, J. Chem. Phys. **18**, 1561 (1950).
  - [36] D. Baeriswyl *et al.*, Phys. Rev. Lett. **56**, 1509 (1986).
  - [37] J. Nilsson *et al.*, Phys. Rev. Lett. **98**, 126801 (2007); arXiv:0712.3259v2.
  - [38] Y.-M. Lin and P. Avouris, arXiv:0801.4576v1.
  - [39] S. V. Morozov *et al.*, Phys. Rev. Lett. **100**, 016602 (2008).
  - [40] E. McCann *et al.*, Phys. Rev. Lett. **96**, 086805 (2006).